Available online at www.sciencedirect.com
SCIENCE DIRECT
Journal of Photochemistry and Photobiology A: Chemistry 181 (2006) 215–225
Journal of Photochemistry and Photobiology A:Chemistry
www.elsevier.com/locate/jphotochem

Fluorescence signaling systems with a cryptand receptor incorporating electron-withdrawing groups: Metal ion specificity and solvent dependence

Bamaprasad Bag, Pritam Mukhopadhyay, Parimal K. Bharadwaj *

Department of Chemistry, Indian Institute of Technology Kanpur, Kanpur 208016, India

Received 28 August 2005; received in revised form 9 November 2005; accepted 1 December 2005
Available online 6 January 2006

Abstract

Fluorescence signaling systems have been synthesized in the format, 'fluorophore-spacer-receptor' or 'receptor-spacer-fluorophore-spacer-receptor' with a laterally non-symmetric aza cryptand as the receptor and anthracene as the fluorophore. Attachment of electron-withdrawing 2,4-dinitrobenzene or 4-nitrobenzene groups as the side-arms of the cryptand imparts structural rigidity to the cryptand core that leads to selective fluorescence enhancement in presence of a metal ion higher in the Irving–Williams series. The present group of compounds exhibit enhancement selectively in presence of Cu(II) as the input. Additionally, an exciplex emission is also observed due to controlled movement of one of the electron-withdrawing side arms towards anthracene forming π–π stacking interactions. The use of MeCN as the solvent is also crucial as in other solvents no emission takes place.

Keywords: Fluorescence enhancement; Metal ion specificity; Cryptand receptors; Exciplex emission

1. Introduction

Fluorescence signaling of metal ions can be useful in a variety of applications such as fluorosensors in biomedical/environmental research, as chemical logics in molecular-scale arithmetic, and so on. Such systems usually comprise of a receptor with one or more N donors covalently linked to a fluorophore either via a spacer or integrated into one unit. The fluorophore and the receptor are chosen such that the operative inter-component process, i.e. intra-molecular photoinduced electron transfer (PET) from the receptor (usually a group containing one or more nitrogen atoms) to the fluorophore can be modulated. When the receptor is empty, PET from the receptor (i.e., N lone-pair) to the excited fluorophore takes place causing a non-radiative decay of the excited state and fluorescence quenching. However, when a metal ion used as input to the receptor, engages this lone-pair by bonding, the PET is blocked causing recovery of the fluorescence. Transition metal ions are ubiquitous in nature and their detection is, therefore, important from biological, clinical as well as environmental aspects. Besides, availability of various redox-states of a transition metal ion can be useful in fabricating molecular photonic devices although transition metal ions generally do not cause recovery of fluorescence due to their quenching nature that prevails over the blockade of the PET process. To circumvent this problem of quenching, it is necessary to have an architectural design where the metal–receptor interaction is high and at the same time, the metal–fluorophore communication is low. Earlier, we had shown [1,2] that when a paramagnetic metal is entrapped inside the cavity of a cryptand, the metal–fluorophore interaction is minimum leading to significant enhancement of fluorescence. However, no specificity in metal ion induced enhancement was observed due to poor chemoselectivity of the receptors [3,4]. Among transition metal ions, Cu(II) has shown toxic impact on several microorganisms even at submicromolar concentration although it is an essential element in a vast majority of bio-systems. Thus, selective fluorescence probes for Cu(II) has attracted attention [5,6] exploiting its high affinity towards N and O donor ligands and fast metal–ligand binding kinetics.

* Corresponding author. Tel.: +91 512 2597340.
E-mail address: pkb@iitk.ac.in (P.K. Bharadwaj).

1010-6030/$ – see front matter © 2005 Elsevier B.V. All rights reserved.
doi:10.1016/j.jphotochem.2005.12.001

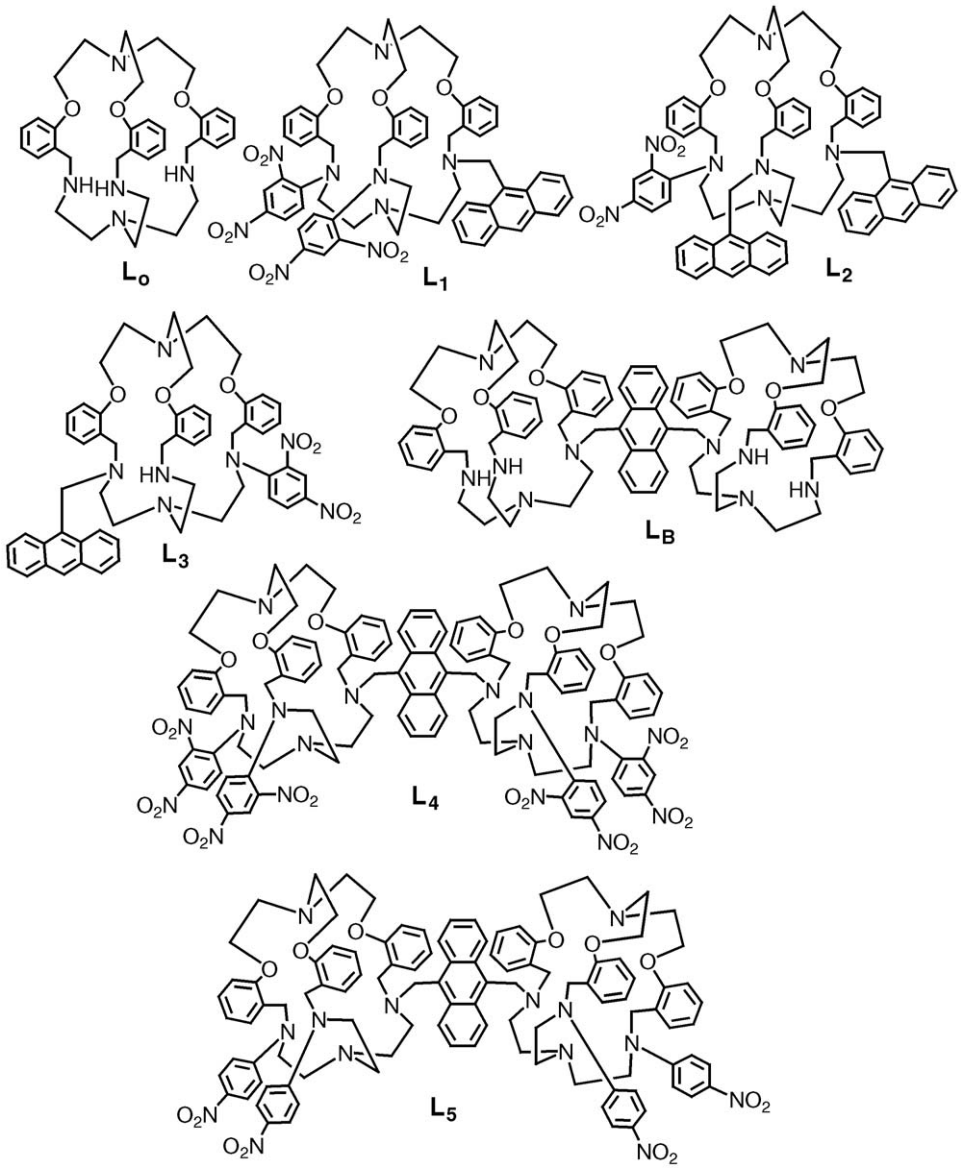

Fig. 1. Chemical structures of the fluorescence signaling systems $\mathbf{L}_1$–$\mathbf{L}_5$.

Molecules exhibiting controlled movements of its parts due to external stimuli such as pH, temperature, photons, redox potential, metal ions and so on, can be important in designing molecular machines [7,8]. In a recent communication [9], we described the synthesis and photophysical studies of two fluorescence signaling systems with a cryptand receptor where attachment of electron-withdrawing 2,4-dinitrobenzene group(s) to the receptor caused selective enhancement with Cu(II) associated with a controlled movement of one of the cryptand arms. In order to probe these effects further, we have synthesized the compounds $\mathbf{L}_1$–$\mathbf{L}_5$ (Fig. 1) built either in 'fluorophore-spacer-receptor' or 'receptor-spacer-fluorophore-spacer-receptor' format and studied their photophysical behavior. Structural rigidity of the receptor core is varied through attachment of different π-acceptors at various positions.

2. Experimental section

2.1. Analysis and measurements

The compounds were characterized by elemental analyses, ^{1}H NMR, ^{13}C NMR and mass (positive ion) spectroscopy. ^{1}H NMR and ^{13}C NMR spectra were recorded on a JEOL JNM-LA400 FT (400 and 100 MHz, respectively) instrument in $CDCl_3$ with Me_4Si as the internal standard. FAB mass (positive ion) data were recorded on a JEOL SX 102/DA-6000 mass spectrometer using argon as the FAB gas at 6 kV and 10 mA with an accelerating voltage of 10 kV and the spectra were recorded at 298 K. ESI mass spectra were recorded on a MICROMASS QUATTRO Quadruple Mass Spectrometer. The samples, dissolved in MeCN were introduced into the ESI source through a syringe pump at the rate of 5 μl/min. The

ESI capillary was set at 3.5 kV and the cone voltage was 40 V, 6 s scan, spectra average 6–8 scans. Melting points were determined with an electrical melting point apparatus by PERFIT, India and were uncorrected. Elemental analyses were done in an Elementar Vario EL III Carlo Erba 1108 elemental analyzer. UV–vis spectra were recorded on a JASCO V-570 spectrophotometer at 298 K in 10^{-4}–10^{-6} M concentration. Steady-state fluorescence spectra were obtained with a Perkin-Elmer LS 50B Luminescence Spectrometer at 298 K ($\sim 10^{-6}$ M). Fluorescence quantum yield was determined in each case by comparing the corrected spectrum with that of anthracene [1] in ethanol by taking the area under the total emission. The quantum yield of anthracene was measured using quinine sulfate in 1N H_2SO_4 [10] at λ_{ex} of 350 nm. The standard quantum yield value thus obtained was used for the calculation of the quantum yield of the samples. The solid-state emission spectra were recorded in a Fluorolog3, model FL3-22, SPEX spectrometer excited at 350 nm with 450 W Xenon lamp, band pass 2 nm and slapped through 1 nm while recording the spectra, integration time was 0.2 s.

2.2. Materials

All the reagent grade chemicals were used without purification unless otherwise specified. 9-Anthracene methanol, 1-chloro-2,4-dinitrobenzene, 1-fluoro-4-nitrobenzene, triethanolamine, salicylaldehyde, tris(2-aminoethyl)amine, sodium borohydride and the metal salts were obtained from Aldrich (US) and used as received. Sodium Hydroxide, anhydrous sodium sulfate, potassium carbonate, perchloric acid and thionyl chloride were received from S. D. Fine Chemicals (India). Thionyl chloride and all the solvents were freshly distilled prior to use and all the reactions were carried out under N_2 atmosphere. Chromatographic separations were done by column chromatography using silica gel (100–200 mesh) obtained from Acme Synthetic Chemicals.

2.3. Synthesis

2.3.1. Synthesis of the cryptand L_0

Cryptand $\mathbf{L_0}$ was synthesized following our method reported earlier [11].

2.3.2. Synthesis of 1a, 1b and 1c

The parent cryptand $\mathbf{L_0}$ was partially derivatized by allowing it to react with the electron-withdrawing 2,4-dinitro-1-chlorobenzene in 1:1.8 molar ratio to obtain tris-, bis- and mono-derivatized (**1a**, **1b**, **1c**) products [12]. The fluorophoric systems $\mathbf{L_1}$, $\mathbf{L_2}$ and $\mathbf{L_3}$ were synthesized by functionalization of **1b** and **1c** with 9-bromomethyl anthracene [13] at different proportions.

The synthetic routes to these ligands are given in Scheme 1.

2.3.3. Synthesis of L_1

The ligand $\mathbf{L_1}$ was synthesized as reported earlier [9] by derivatization of **1b** with 9-bromomethyl anthracene.

2.3.4. Synthesis of L_2 and L_3

The ligand $\mathbf{L_2}$ was also synthesized as reported earlier [9] by derivatization of **1c** with two equivalents of 9-bromomethyl anthracene. In another route as described below, derivatization of **1c** with 1.3 equivalents of 9-bromomethyl anthracene yields a mixture of both $\mathbf{L_2}$ and $\mathbf{L_3}$ affording substantial yields of the desired products which were subsequently separated through column chromatography.

To a solution of **1c** (0.73 g, 1 mmol) in dry acetonitrile (50 mL), K_2CO_3 (0.42 g, 3 mmol) was added and stirred for 15 min under dinitrogen atmosphere. To this, 9-(bromomethyl) anthracene (0.35 g, 1.3 mmol) was added followed by a crystal of KI and the mixture allowed to reflux for 48 h. After removing the solvent in a rotary evaporator, water (50 mL) was added to it and the desired compounds were extracted with dichloromethane (3×50 mL). After drying the organic layer over anhydrous Na_2SO_4, it was evaporated to dryness to obtain a yellow solid

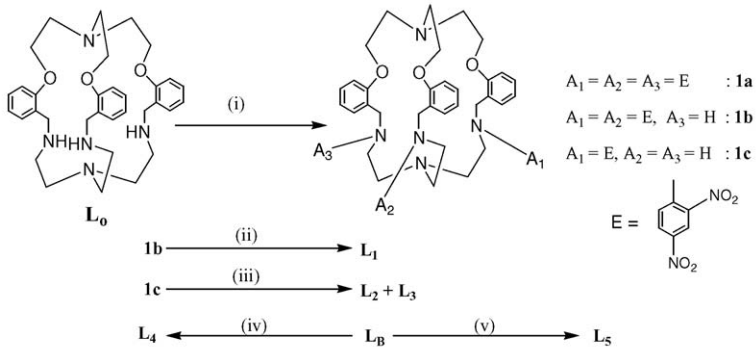

Reaction conditions: (i) 2,4-dinitro-1-chlorobenzene(1.8 eq.), EtOH, K_2CO_3, reflux, 6h. (ii)&(iii) 9-bromomethyl anthracene(1.0 eq. for (ii) and 1.3 eq. for (iii)), K_2CO_3, KI, MeCN, reflux, 48 h. (iv) 2,4-dinitro-1-chlorobenzene(4.0 eq.), EtOH, K_2CO_3, Reflux, 8h.(v) 1-fluoro-4-nitrobenzene(4.0 eq.), DMSO, K_2CO_3, 70 °C, 48h.

Scheme 1. Synthetic route to the ligands $\mathbf{L_1}$–$\mathbf{L_5}$.

residue that was a mixture of $\mathbf{L}_2$ and $\mathbf{L}_3$. They were separated by column chromatography (silica gel, 100–200 mesh) with $CHCl_3$ and MeOH mixture as eluent.

Ligand $\boldsymbol{L_2}$: The first compound separated from the column with $CHCl_3$ and MeOH mixture (98:2 v/v) as the eluent was characterized as $\mathbf{L}_2$. Recrystallization from MeOH: dichloromethane mixture afforded an orange solid. X-ray quality, rectangular parallelepiped crystals were grown by slow evaporation from dichloromethane–ethyl acetate mixture.

Yield: 0.64 g (58%); M. pt.: 183 °C; ^{1}H NMR (400 MHz, $CDCl_3$, 25 °C, TMS) δ: 2.14 (s, 4H); 2.29 (s, 4H), 2.76 (d, J = 8.35 Hz, 4H), 3.09 (br s, 4H), 3.59 (s, 2H), 4.31 (br s, 12H), 4.87 (d, 4H), 6.67 (d, 1H), 6.76–6.83 (m, 10H), 7.09 (m, 12H), 7.41 (br, s, 6H), 7.89 (dd, J = 8.25 Hz, J = 2.0 Hz, 1H), 8.11 (br, s, 2H), 8.24 (s, 1H); ^{13}C NMR (100 MHz, $CDCl_3$, 25 °C, TMS) δ: 154, 139, 131–120, 117, 110, 67, 57, 54, 52, 51; FAB-MS, *m/z* (%): 1106 (100) $[\mathbf{L}_2]^+$; Anal. Calcd for $C_{69}H_{67}N_7O_7$: C, 74.91; H, 6.1; N, 8.86%. Found: C, 74.63; H, 6.13; N, 8.71%.

Ligand $\boldsymbol{L_3}$: The fraction was eluted out from the column using dichloromethane: methanol in the ratio of 93:7 (v/v) as the eluent was characterized as $\mathbf{L}_3$. The yellow product isolated was recrystallized from acetone to obtain a yellow crystalline solid.

Yield: 0.32 g (35%); M. pt.: 139 °C; ^{1}H NMR (400 MHz, $CDCl_3$, 25 °C, TMS) δ: 2.08 (s, 2H), 2.23 (d, J = 8.35 Hz, 4H), 2.63 (s, 2H), 2.69 (s, 4H), 3.01 (br s, 1H), 3.19 (br s, 4H), 3.54 (s, 2H), 4.14 (br s, 6H), 4.40 (s, 6H), 4.45 (s, 2H), 6.42 (d, J = 9.27 Hz, 1H), 6.66 (br s, 3H), 6.82 (br s, 3H), 7.01 (d, J = 6.83 Hz, 3H), 7.11(t, J = 7.07 Hz, 3H), 7.29 (m, aromatic, 4H), 7.72 (d, J = 8.79 Hz, 2H), 7.79 (d, J = 7.31 Hz, 1H), 8.08 (s, 1H), 8.17 (d, J = 8.55 Hz, 2H), 8.38 (s, 1H); ^{13}C NMR (100 MHz, $CDCl_3$, 25 °C, TMS) δ: 159, 140, 134–121, 116, 115, 114, 68, 58, 56, 51, 49, 44; ESI-MS, *m/z* (%): 919 (46) $[\mathbf{L}_3 + \mathbf{3}]^+$; Anal. Calcd. for $C_{54}H_{57}N_7O_7$: C, 70.80; H, 6.26; N, 10.70%. Found: C, 70.63; H, 6.38; N, 10.54%.

2.3.5. Synthesis of the bis-cryptand, $\boldsymbol{L_B}$

Synthesis of $\mathbf{L}_B$ [14] was achieved as reported earlier from our laboratory.

2.3.6. Synthesis of $\boldsymbol{L_4}$

To a suspension of $\mathbf{L}_B$ (0.66 g, 0.5 mmol) in dry EtOH (50 mL) was added anhydrous K_2CO_3 (0.3 g, 2.1 mmol) and the reaction mixture was stirred for 10 min. Subsequently, a solution of 1-chloro-2,4-dinitrobenzene (0.41 g, 2 mmol) in dry EtOH (10 mL) was added dropwise for 15 min and the reaction mixture was allowed to stir at RT for 2 h during which the solution became yellow-orange in color. It was allowed to reflux for 8 h. After cooling to RT, the solvent was removed in a rotary evaporator and the yellow solid obtained was repeatedly washed with water (5 × 100 mL). The desired product was purified and isolated as an orange solid by passing through silica gel column (100–200 mesh) with dichloromethane–ethylacetate mixture (90:10 v/v) as the eluent. This product crystallizes as orange block-shaped single crystals [15] suitable for X-ray crystallography by slow evaporation of its solution in chloroform and tricholoethylene.

Yield: 0.84 g (83%); M. pt.: 172 °C; ^{1}H NMR (400 MHz, $CDCl_3$, TMS, 25 °C) δ: 1.18 (t, J = 7.31 Hz, 4H), 1.97 (s, 4H), 2.03 (br s, 8H), 2.17 (s, 8H), 2.54 (m, 4H), 2.67 (m, 4H), 3.17 (br s, 8H), 3.47 (s, 8H), 4.05 (m, 8H), 4.41 (s, 4H), 4.45 (s, 4H), 6.40 (d, J = 9.51 Hz, 6H), 6.59 (t, J = 7.31 Hz, 6H), 6.68 (d, J = 8.07 Hz, 4H), 6.73–6.89 (m, 6H), 6.92 (d, J = 6.83 Hz, 6H), 7.14 (m, 4H), 7.25 (dd, J = 2.91 Hz, 6.89 Hz, 2H), 7.74 (dd, J = 2.68 Hz, 6.83 Hz, 2H), 8.16 (dd, J = 2.95 Hz, 6.93 Hz, 4H), 8.39 (s, 4H); ^{13}C NMR (100 MHz, $CDCl_3$, 25 °C, TMS) δ: (aromatic) 156.28, 136.66, 130.72, 129.06, 128.24, 127.19, 125.52, 123.56, 123.15, 118.05, 110.94, (aliphatic) 67.25, 66.48, 60.40, 54.77, 50.53, 14.18; ESI-MS, *m/z* (%): 1987(67) $[\mathbf{L}_4 + 1]^+$, 2023 (12) $[\mathbf{L}_4 + 2H_2O]^+$, Anal. Calcd. for $C_{106}H_{108}N_{18}O_{22}$ [1986.13]: C, 64.10; H, 5.48; N, 12.69%. Found: C, 64.03; H, 5.53; N, 12.60%.

2.3.7. Synthesis of $\boldsymbol{L_5}$

To a stirring solution of $\mathbf{L}_B$ (0.66 g, 0.5 mmol) in dry DMSO (15 mL), anhydrous K_2CO_3 (0.30 g, 2.1 mmol) was added. Subsequently, 1-fluoro-4-nitrobenzene (0.28 g, 2 mmol) was added in dry DMSO (15 mL) was added dropwise in 30 min and the reaction mixture was allowed to stir at 70 °C for 48 h. The reaction mixture was then poured into cold water (250 mL). The yellow solid separated, was collected by filtration and washed thoroughly with water (5 × 100 mL) and air-dried. The desired product was purified and isolated as an orange solid by passing through a silica gel column (100–200 mesh) with dichloromethane–ethylacetate mixture (70:30 v/v) as the eluent.

Yield: 0.68 g (75%); M. pt.: 196 °C; ^{1}H NMR (400 MHz, $CDCl_3$, TMS, 25 °C) δ: 0.8 (m, 4H), 1.18 (s, 4H), 2.09 (br d, 4H), 2.22 (br s, 6H), 2.47 (br s, 4H), 2.77 (br s, 6H), 2.91 (br d, 6H), 3.12 (br d, 6H), 3.21 (br s, 6H), 3.58 (s, 4H), 4.01 (s, 4H), 4.12 (s, 4H), 4.30 (m, 8H), 6.04 (d, J = 8.75 Hz, 6H), 6.48 (d, J = 7.03 Hz, 4H), 6.57–6.69 (m, 4H), 6.80 (d, J = 8.27 Hz, 4H), 6.99 (br d, 4H), 7.04 (br d, 4H), 7.12 (t, J = 7.55 Hz, 6H), 7.18–7.21 (m, 4H), 7.60 (t, J = 7.59 Hz, 4H), 8.14 (s, 4H), 8.53 (s, 4H); ^{13}C NMR (100 MHz, $CDCl_3$, 25 °C, TMS) (: (aromatic) 157.02, 155.91, 152.41, 149.65, 136.50, 136.04, 130.58, 128.18, 126.42, 125.89, 125.29, 124.68, 124.41, 123.73, 120.72, 111.00, 110.00, (aliphatic) 66.72, 53.60 52.84, 50.64, 49.40, 29.62; ESI-MS, *m/z* (%): 1807(77) $[\mathbf{L}_5 + 1]^+$, Anal. Calcd for $C_{106}H_{112}N_{14}O_{14}$ [1806.14]: C, 70.49; H, 6.25; N, 10.86%. Found: C, 70.40; H, 6.37; N, 10.81%.

2.3.8. General synthesis of Cu-complex of $\boldsymbol{L_1}$–$\boldsymbol{L_5}$

To a stirring solution of a ligand (0.1 mmol) in dry ethanol, an ethanolic solution of $Cu(ClO_4)_2 \cdot 6H_2O$ (0.1 mmol) was added followed by NaCl (0.1 mmol) and stirred for 2 h at RT till the color of the solution turned green. After filtration, the filtrate left at RT overnight affords a green crystalline solid as the desired product. The solid was collected by filtration, washed and dried under vacuum for further use in solid-state emission measurements.

2.3.9. General synthesis of protonated L_1–L_5

To a stirring solution of a ligand (0.1 mmol) in acetonitrile, dilute perchloric acid solution was added and stirred for 2 h at RT and filtered off. The filtrate was left at RT for 3–4 days to afford deep yellow block-shaped crystals for protonated $\mathbf{L}_1$ and $\mathbf{L}_2$ where as a brownish crystalline solid obtained as the desired protonated species of other ligands. The solid was collected by filtration, washed and dried under vacuum for further use.

3. Results and discussion

3.1. Crystallographic structural studies

Structural studies [15] of three compounds, viz., $\mathbf{L}_1$, $\mathbf{L}_2$ and $\mathbf{L}_4$ (Fig. 1) were carried out at 100 K. Crystallization of the remaining compounds were unsuccessful. The structure of $\mathbf{L}_1$ and $\mathbf{L}_2$ were reported earlier [9]. A perspective view of the structure of $\mathbf{L}_4$ is shown in Fig. 2.

In each case, the cryptand core has an endo–endo conformation and the distance between the two bridgehead N atoms varies from 6.392 Å in $\mathbf{L}_1$ to 5.680 Å in $\mathbf{L}_4$ in comparison to 6.272 Å in the parent cryptand $\mathbf{L}_0$ [11]. The non-bonding distances between the amino N as well as the ethereal O atoms are larger [15] compared to the corresponding distances in $\mathbf{L}_0$. Thus, increasing the number of 2,4-dinitrobenzene moieties causes the cavity to bulge, and contributes significantly towards stereo-electronic situation in these systems. Also, the N–C bond between the cryptand and the phenyl ring of the 2,4-dinitrobenzene group is significantly shorter (1.356–1.374 Å) compared to normal C–N bond length [11]. This causes partial double bond character and restricted rotation of the 2,4-dinitrobenzene moiety that assumes different orientation with respect to the cryptand in the three structures. The partial double bonding also indicates delocalization of electron density from the N atom of the cryptand to the π-cloud of 2,4-dinitrobenzene.

3.2. UV–vis absorption spectroscopy of the ligands

The absorption spectra (Fig. 3a) of these ligands in different solvents are found to be overlapping of two transitions in the 340–450 nm region, (i) anthracence $S_0 \rightarrow S_1$ along with Frank–Condon vibrational structures, and (ii) intramolecular charge transfer (ICT) from donor N atom to the acceptor nitro groups [16] through the π spacer. The band at ∼260 nm is attributable [17] to the π–π interaction between the phenyl of the side-groups and the anthracence in the ground state along with anthracence $S_0 \rightarrow S_3$ transition. In $\mathbf{L}_1$–$\mathbf{L}_4$, these transitions are found to be non-solvatochromic in nature. However, in $\mathbf{L}_5$, the first of the above two transitions is slightly red shifted (λ_{max} = 402 nm in DMSO in comparison to λ_{max} = 376 nm in THF) with increase in solvent polarity (Fig. 3b).

3.3. Absorption in presence of transition metal ions

Upon complexation with a metal ion, a small shift ($\Delta\lambda$ = 2–5 nm in MeCN) of the absorption band with concomitant decrease in molar extinction coefficient (ε) is observed for all the systems. The absorption spectral pattern in each case remains the same, except in presence of Cu(II) where the Frank–Condon vibrational structures shift towards higher energy region (Fig. 4). This is indicative of a different binding mode towards Cu(II) ion compared to other metal ions.

Protonation of $\mathbf{L}_1$ and $\mathbf{L}_4$ is associated with large increase in molar extinction coefficient (ε) as well as blue-shift of the

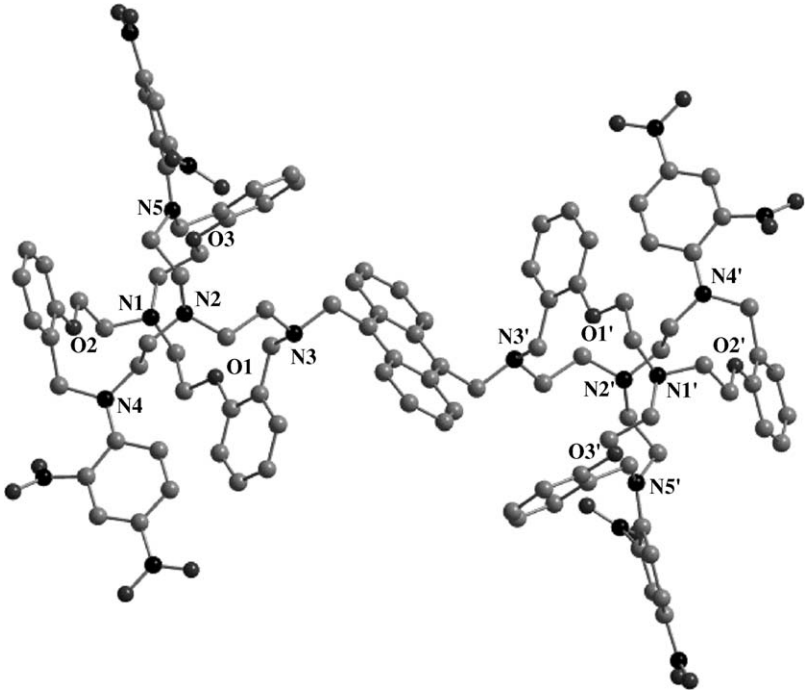

Fig. 2. Perspective view of the crystal structure of $\mathbf{L}_4$.

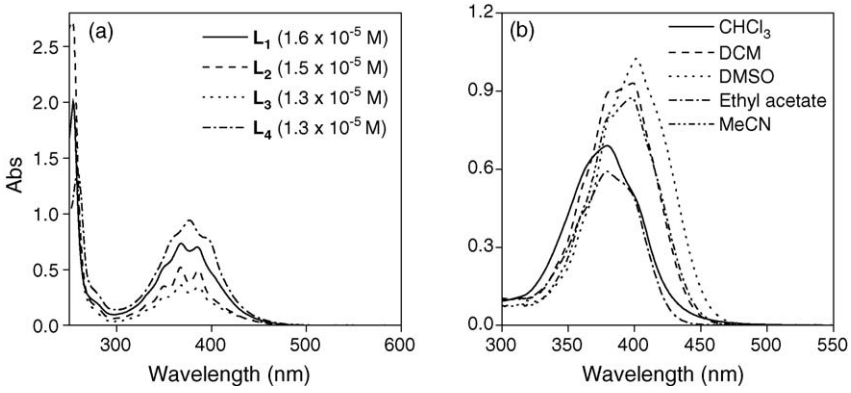

Fig. 3. Absorption spectra of (a) $\mathbf{L}_1$–$\mathbf{L}_4$ in MeCN (conc. = 1×10^{-5} M) and (b) $\mathbf{L}_5$ in different solvents (conc. = 1×10^{-5} M).

absorption transitions in the visible region (Fig. 4), which are the characteristics of increased charge transfer process [18]. This behavior is more pronounced in $\mathbf{L}_4$ than that in $\mathbf{L}_1$, presumably due to the presence of more numbers of electron-withdrawing 2,4-dinitrobenzene groups in the former. Absorption spectral features of protonated $\mathbf{L}_2$, $\mathbf{L}_3$ and $\mathbf{L}_5$ remain the same with concomitant decrease in ε, as observed with other metal ions except Cu(II).

3.4. Emission behavior of the cation free systems

The cation free $\mathbf{L}_1$–$\mathbf{L}_5$ show well-resolved anthracene monomer emission at 298 K in all the solvents under investigation. The ICT operative here from the donor amino N atom to the acceptor nitro moiety through a π spacer is found to be non-emitting [12] in nature. The structured non-solvatochromic anthracence emission of $\mathbf{L}_1$ was observed with (0, 0) band centered at ∼395 nm along with vibrational structures at 412 and 440 nm. Interestingly, the emission of $\mathbf{L}_2$ is found to be solvatochromic in nature. Emission maxima (λ_{max}) typical of anthracence of $\mathbf{L}_2$ is observed at 430 nm in non-polar dichloromethane which is ∼20 nm blue-shifted in relatively polar DMSO/DMF.

However, none of the systems except $\mathbf{L}_3$ show any exciplex formation that appears as a structureless broad band around 550 nm that was found in case of the tris-anthryl derivatives of $\mathbf{L}_0$. The restricted orbital orientation of the donor N atom with the fluorophore due to imposed structural rigidity to the cryptand core upon attachment of electron withdrawing groups causes a poor overlap between them and hence, leads towards an unfavorable condition for exciplex emission. The interference of solvent molecules with more access to the lone pair of the N atom bound to the fluorophore also prohibits the exciplex formation. However, $\mathbf{L}_2$ exhibit a red shifted band ∼540 nm in non-polar DCM attributed to the exciplex formation which is not observed in other comparatively polar solvents.

Cation free $\mathbf{L}_3$ shows dual emission consist of a well resolved anthracene monomer emission with (0, 0) emission band at 394 nm corresponding to locally excited $^1(\pi$–$\pi^*)$ state along with a red-shifted broad structureless emission centered at 542 nm in DCM at 298 K (Fig. 5). The excitation spectra monitoring the (0, 0) band of the structured emission and the λ_{max} of band are broad emission are identical and match well with the absorption spectra of $\mathbf{L}_3$ in almost all non-polar solvents under investigation, this overrules [19] formation of any ground state complexes. The position of the structureless broad emission is found to be sensitive towards solvent polarity showing the charge transfer character of the emitting complex. The emission band is red-shifted with increase in solvent polarity, this ascertains that it is due to intramolecular exciplex [20] formation not due to excimer formation. A linear relationship was observed when

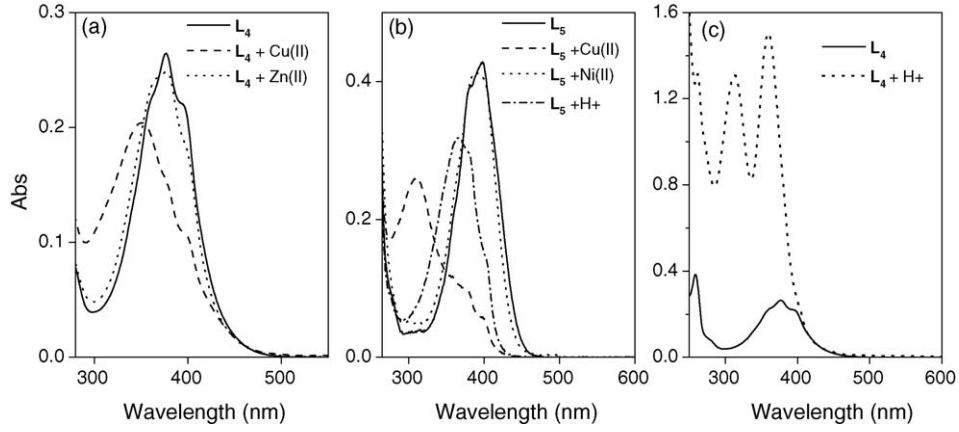

Fig. 4. Absorption spectra of (a) $\mathbf{L}_4$ (conc. = 3.6×10^{-6} M), (b) $\mathbf{L}_5$ (conc. = 4.9×10^{-6} M), in the presence of different ionic inputs and (c) $\mathbf{L}_4$ (conc. = 3.6×10^{-6} M) in presence of H^+.

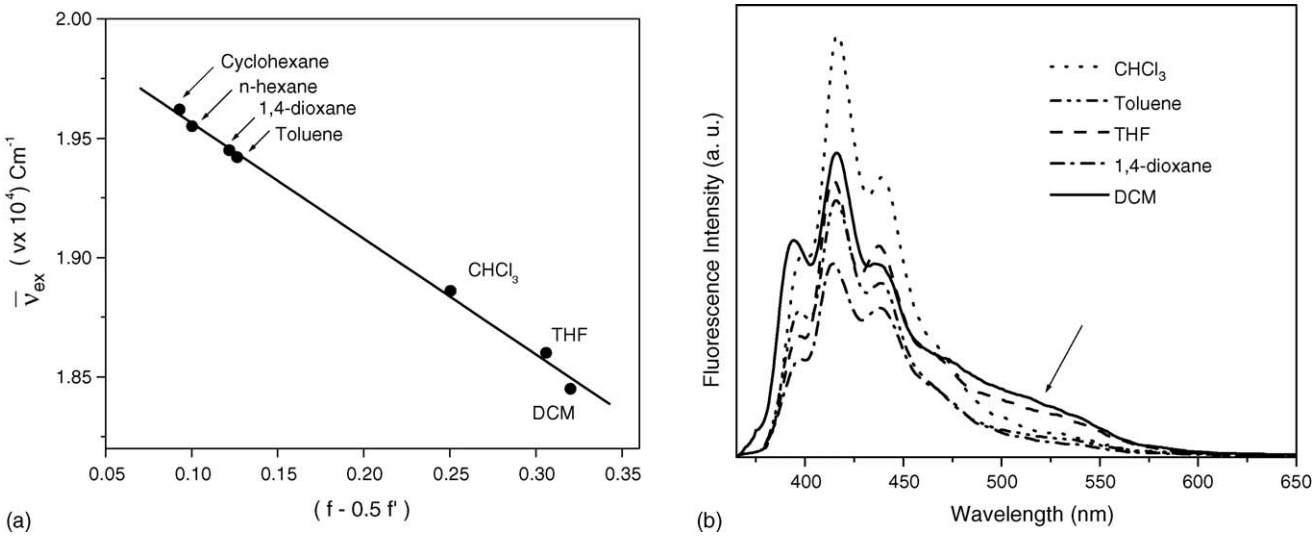

Fig. 5. (a) ν_{ex} of the exciplex emission maximum of $\mathbf{L}_3$ at 298 K as a function of solvent polarity parameter $f-0.5f'$ where $f=(\varepsilon-1)/(2\varepsilon+1)$ and $f'=(\eta^2-1)/(2\eta^2+1)$. (b) Fluorescence spectral pattern of $\mathbf{L}_3$ in different solvents.

ν_{ex} (max) is plotted (Fig. 5) against solvent polarity parameter [21] is in consistent with the Weller's equation, i.e.

$$\nu_{ex} = \nu_{ex}(0) - (2\mu_{ex}^2/hc\rho^3)(f - 0.5f') \quad (1)$$

where ν_{ex} (cm^{-1}) is the fluorescence maximum of exciplex emission in a given solvent, $\nu_{ex}(0)$ is that in vacuum, μ_{ex} the dipole moment of the exciplex, ρ the radius of the solvent cavity, $(f-0.5f')$ is the solvent polarity parameter measured from its dielectric constant (ε) and refractive index (η) [$f=(\varepsilon-1)/(2\varepsilon+1)$ and $f'=(\eta^2-1)/(2\eta^2+1)$]. The solvent polarity parameters, λ_{ex} (nm) and ν_{ex} in various solvents are collected in Table 1.

On the basis of the plot, derived from the above Weller's equation, the excited state dipole moment μ_{ex} for $\mathbf{L}_3$ is found to be 28 D, using the solvent sphere having a diameter $\rho \cong 5.5$ Å. The values obtained for the intramolecular exciplexes in tris-anthracene substituted $\mathbf{L}_0$ was ~10 D. In $\mathbf{L}_3$, the high value of μ_{ex} indicates that complete charge transfer occurs in the excited state. The values of μ_{ex} obtained based on several approximation and should be considered as tentative. However, the dipole moments depend upon the distance between the donor N atom and the aromatic hydrocarbon, i.e. the anthracence. The extent of charge transfer in this kind of exciplex depends upon the extent of overlap of the lone pair of donor N atom and the π electrons of anthracence. The high value of μ_{ex} for $\mathbf{L}_3$ indicative of a complete charge transfer character of the broad emission observed.

Table 1
ν_{ex} as a function of solvent polarity parameter $(f-0.5f')$ in $\mathbf{L}_3$

Solvents	ε	η	$f-0.5f'$	λ_{ex} (nm)	ν_{ex} ($\times 10^4$) cm^{-1}
Cyclohexane	2.02	1.426	0.0931	510	1.961
n-Hexane	1.89	1.375	0.1004	512	1.953
1,4-Dioxane	2.21	1.422	0.1219	514	1.946
Toluene	2.38	1.496	0.1265	515	1.942
$CHCl_3$	4.70	1.446	0.2505	530	1.887
THF	7.32	1.407	0.3053	537	1.862
DCM	8.90	1.424	0.3201	542	1.845

The fluorescence quantum yield (ϕ_F) of these systems is found to be more in non-polar than in polar solvents. This is because, the PET process is considerably enhanced in polar medium due to charge-dipole and H-bonding interactions causing lower fluorescence quantum yield [22]. The quantum yield ϕ_F is found to be extremely low in metal-free systems attributable to a highly efficient PET process operative between the HOMO of the donor tertiary N atom and the anthracene π systems. The absorption maxima (λ_{max}^{abs}), fluorescence maxima (λ_{max}^{em}) and quantum yields (ϕ_F) of $\mathbf{L}_1$–$\mathbf{L}_5$ in different solvents are given in Table 2.

3.5. Emission characteristics in presence of metal ions

In presence of Cu(II) ion, $\mathbf{L}_1$–$\mathbf{L}_5$ exhibit fluorescence enhancement up to ~180-fold in acetonitrile while other transition metal ions probed do not show this behavior (Table 3). Compound $\mathbf{L}_5$ behaves somewhat differently showing fluorescence enhancement in presence of Tl(III) as well (Fig. 6a). In each case, fluorescence enhancement is accompanied by appreciable red-shift of the (0, 0) band along with a different intensity ratio for the (0, 0) and the first vibrational bands. The compound $\mathbf{L}_5$ exhibits maximum red-shift with Cu(II) in MeCN. This red-shift is attributable to the change in polarity around the fluorophore whose emission band is solvatochromic in nature.

Low fluorescence recovery in presence of a transition metal ion other than Cu(II) is presumed to be due to lack of proper bonding interactions. Attachment of electron-withdrawing groups lowers donating ability of the cryptand and only Cu(II) forms stable complexes in preference over others following the Irving–Williams order of stability [23]. Such behavior was observed earlier in aza-macrocycle [24] and aza-cyclophane [25] based receptors. The plot of fluorescence

Table 2
Absorption maxima, emission maxima and fluorescence quantum yield (ϕ_F) of $\mathbf{L}_1$–$\mathbf{L}_5$ in different solvents

Fluorophoric systems	Solvents	λ_{abs}^{max} (nm)	λ_{em}^{max} (nm)	ϕ_F
$\mathbf{L}_1$	DCM	369	415	0.0054
	THF	368	410	0.0091
	$CHCl_3$	369	416	0.0020
	Toluene	369	413	0.0013
	MeCN	368	412	0.0011
	dioxane	369	412	0.0007
	Acetone	369	412	0.0003
	DMF	369	413	0.0007
	DMSO	371	412	0.0005
$\mathbf{L}_2$	DCM	369	430	0.0600
	THF	368	414	0.0080
	$CHCl_3$	369	421	0.0200
	Toluene	368	416	0.0047
	MeCN	367	412	0.0013
	dioxane	367	410	0.0014
	Acetone	367	410	0.0019
	DMF	369	409	0.0006
	DMSO	368	409	0.0009
$\mathbf{L}_3$	DCM	369	416	0.0046
	THF	368	413	0.0027
	$CHCl_3$	369	416	0.0025
	Toluene	369	416	0.0042
	MeCN	367	413	0.0053
	dioxane	368	412	0.0024
	Acetone	369	414	0.0029
	DMF	369	413	0.0009
	DMSO	369	412	0.0005
$\mathbf{L}_4$	Chloroform	376	420	0.0029
	DCM	380	421	0.0022
	Toluene	378	421	0.0027
	1,4-Dioxane	377	421	0.0053
	THF	377	420	0.0020
	Acetone	377	420	0.0022
	Acetonitrile	378	419	0.0036
	DMF	378	420	0.0043
	DMSO	380	422	0.0038
$\mathbf{L}_5$	Chloroform	380	430	0.0079
	Toluene	380	427	0.0068
	1,4-Dioxane	379	428	0.0017
	THF	376	429	0.0045
	DCM	399	430	0.0058
	Acetone	397	421	0.0059
	Acetonitrile	398	418	0.0019
	DMF	400	419	0.0032
	DMSO	402	414	0.0022

titrations with Cu(II) in acetonitrile (Fig. 6b) indicate a 1:1 complex formation in $\mathbf{L}_1$–$\mathbf{L}_3$ while it is 2:1 complexation in $\mathbf{L}_4$ and $\mathbf{L}_5$. On protonation, all the compounds exhibit different extents of fluorescence recovery. In order to verify that the fluorescence enhancement is due to the metal ion input not because of protons generated from the metal salts in organic solvents, certain control experiment are carried out as described earlier [1,4]. Thus, attachment of electron-withdrawing 2,4-dinitrobenzene groups to the cryptand core as in $\mathbf{L}_1$–$\mathbf{L}_3$ results in selective Cu(II)-induced fluorescence enhancement in comparison to the tris-, bis- and mono-anthryl substituted cryptand based signaling sys-

Table 3
Absorption maxima, fluorescence maxima, fluorescence quantum yields[a] and fluorescence enhancement factors (FE) for $\mathbf{L}_1$–$\mathbf{L}_5$ in presence of different ionic inputs

Systems	Ionic inputs	λ_{abs}^{max} (nm)	λ_{em}^{max} (nm)	Fluorescence	
				ϕ_F	FE
$\mathbf{L}_1$	–	368	411	0.0011	1
	Mn(II)	369	411	0.0216	20
	Fe(II)	369	412	0.0364	33
	Co(II)	370	412	0.0227	21
	Ni(II)	371	411	0.0221	20
	Cu(II)	353	415	0.1778	162
	Zn(II)	371	412	0.0385	35
	Cd(II)	371	412	0.0242	22
	Ag(I)	368	411	0.0451	41
	Pb(II)	368	412	0.0289	26
	Hg(II)	367	411	0.0034	3
	H^+	314	414	0.0972	88
$\mathbf{L}_2$	–	367	412	0.0013	1
	Mn(II)	368	412	0.0173	13
	Fe(II)	371	412	0.0197	15
	Co(II)	368	413	0.0320	25
	Ni(II)	368	413	0.0312	24
	Cu(II)	351	416	0.1632	126
	Zn(II)	371	413	0.0370	29
	Cd(II)	372	413	0.0352	27
	Ag(I)	368	413	0.0391	30
	Pb(II)	368	412	0.0259	20
	Hg(II)	368	412	0.0074	6
	H^+	351	417	0.1924	148
$\mathbf{L}_3$	–	368	401	0.0053	1
	Mn(II)	368	404	0.0474	9
	Fe(II)	367	410	0.1065	20
	Co(II)	369	409	0.0976	18
	Ni(II)	369	410	0.1113	21
	Cu(II)	351	421	0.468	88
	Zn(II)	370	410	0.1151	22
	Cd(II)	370	410	0.1496	28
	Ag(I)	368	412	0.1587	30
	Pb(II)	368	413	0.2179	41
	Hg(II)	368	402	0.0078	1
	H^+	350	414	0.6141	116
$\mathbf{L}_4$	–	378	424	0.0036	1
	Mn(II)	378	425	0.0057	1
	Fe(II)	379	425	0.0081	2
	Co(II)	379	424	0.0039	1
	Ni(II)	378	425	0.0114	3
	Cu(II)	350	441	0.2649	74
	Zn(II)	378	425	0.0039	1
	Cd(II)	379	425	0.0072	2
	Ag(I)	378	425	0.0045	1
	Pb(II)	378	425	0.0036	1
	Hg(II)	377	425	0.0045	1
	H^+	313	430	0.0738	21
$\mathbf{L}_5$	–	398	399	0.0019	1
	Mn(II)	393	401	0.0049	3
	Fe(II)	388	400	0.0046	3
	Co(II)	393	401	0.0052	3
	Ni(II)	390	401	0.0076	4
	Cu(II)	310	429	0.3409	179
	Zn(II)	388	418	0.0467	25
	Cd(II)	391	402	0.0093	5

Table 3 (*Continued*)

Systems	Ionic inputs	λ_{abs}^{max} (nm)	λ_{em}^{max} (nm)	Fluorescence	
				ϕ_F	FE
	Ag(I)	396	422	0.0194	10
	Pb(II)	398	402	0.0037	2
	Tl(III)	396	446	0.1207	64
	H^+	365	423	0.0400	21

[a] Experimental conditions: medium, dry MeCN; concentration of free ligands: $\sim 10^{-6}$ M; concentration of ionic input: $\sim 10^{-5}$ M; $\lambda_{ex} = 350$ nm; excitation and emission band-pass: 5 nm; temperature: 298 K; ϕ_{FT} calculated by comparison of corrected spectrum with that of anthracene ($\phi_F = 0.297$) taking the area under the total emission. The error in ϕ_F is within 10% for the free ligand, otherwise 5% in each case.

tems [1,4] where no specificity towards metal ions was obtained. Similarly, although $\mathbf{L}_B$ [14] exhibits versatility in fluorescence enhancement in presence of many transition as well as heavy metal ions, attachment of electron-withdrawing substituents to its cryptand cores ($\mathbf{L}_4$–$\mathbf{L}_5$) brings about selective fluorescence recovery in presence of Cu(II) in comparison to other transition metal ions investigated.

3.6. Exciplex emission and structure–function correlation

In the fluorescence spectra of $\mathbf{L}_1$–$\mathbf{L}_5$, no exciplex formation in acetonitrile is observed as the charge transfer states are more stabilized in polar than in non-polar solvents. Interestingly, with Cu(II) and not with any other transition metal ions, a broad structureless emission centered around ~540 nm appears along with the monomer emission (Fig. 7). Of course, compound $\mathbf{L}_5$ that gives enhancement in presence of Tl(III), exhibits a similar band (Fig. 6a) as well. The excitation spectra monitoring both the monomer and the broad emission band in acetonitrile found to be same and matches well with their absorption spectra, indicating the broad emission to be a DA type exciplex [26], that primarily arises due to π-electron interaction of anthracence and the aromatic ring of the attached electron-withdrawing groups. As evidenced from the X-ray crystal structures of protonated $\mathbf{L}_1$ and $\mathbf{L}_2$ [9], a structural rearrangement in these systems occurs upon protonation due to controlled movement of one of the electron-withdrawing side groups towards the anthracene ring making a π–π stacking interaction that causes the exciplex emission. Conformational distortion of the cryptand also takes place [27]

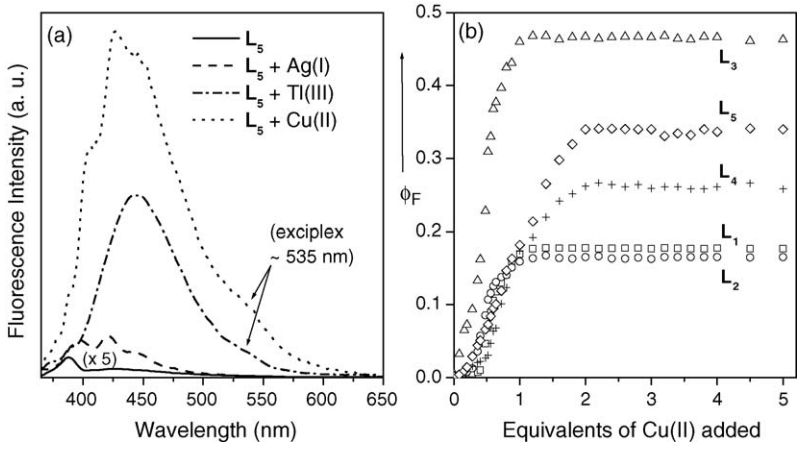

Fig. 6. (a) Corrected fluorescence spectra (in arbitrary intensity scales) of $\mathbf{L}_5$ (5×) alone and in presence of various ionic inputs. The fluorescence quantum yields and corresponding fluorescence enhancement factors of $\mathbf{L}_1$–$\mathbf{L}_5$ in presence of different ionic inputs are given in Table 3. (b) Plot of total fluorescence quantum yield (ϕ_{FT}) as a function of equivalents of Cu(II) added to (□) $\mathbf{L}_1$ (2.5 μM), (◯) $\mathbf{L}_2$ (2.0 μM), (△) $\mathbf{L}_3$ (2.5 μM), (+) $\mathbf{L}_4$ (2.0 μM) and (◇) $\mathbf{L}_5$ (2.5 μM) in MeCN.

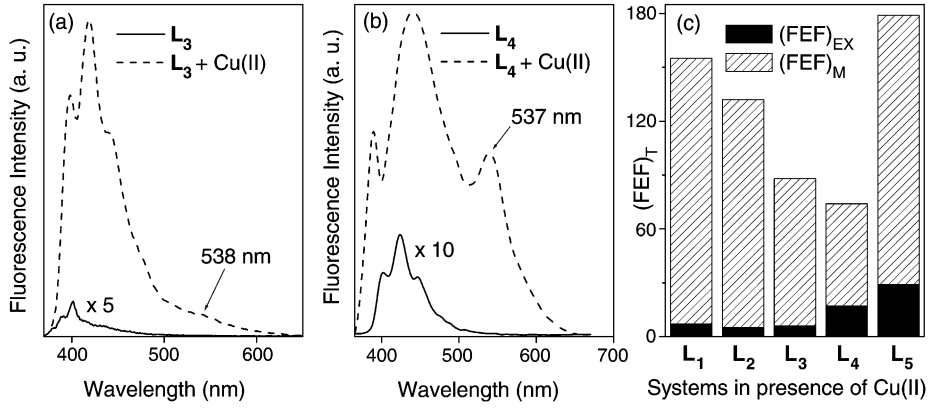

Fig. 7. Fluorescence emission spectra of (a) $\mathbf{L}_3$ (conc. 2.5×10^{-6} M) and (b) $\mathbf{L}_4$ (conc. 2.0×10^{-6} M) in presence of Cu(II) in MeCN. (c) Graphical representation of the total fluorescence enhancement factor $(FEF)_T$ of $\mathbf{L}_1$–$\mathbf{L}_5$ in presence of Cu(II) in MeCN showing their corresponding contributions from monomer enhancement and exciplex emission: $(FEF)_T = (FEF)_M + (FEF)_{EX}$.

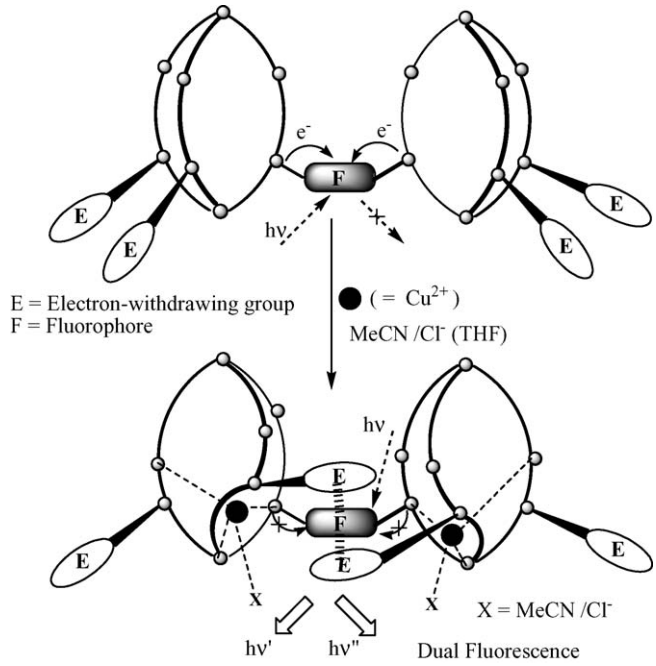

Scheme 2. Schematic representation of the signaling action by the perturbation of the processes involved in these ligands upon Cu(II) complexation in MeCN.

under favorable conditions leading to exocyclic coordination of a metal ion. It follows, therefore, that similar conformational changes take place on binding to Cu(II) or protonation with concomitant movement of one of the side groups.

Interestingly, when emission of these ligands in presence of Cu(II) is probed in different solvents, it is found that both monomer and exciplex emissions are given in MeCN medium only. In poorly coordinating solvents such as CH_2Cl_2, $CHCl_3$, THF, etc., no significant emission takes place. However, addition of MeCN to these solutions results in significantly enhanced monomer and exciplex emissions. Also, these emissions can be observed when Cl^- ion is added to the THF solution. We had earlier shown [27] that a co-ligand, mostly a counter anion like Cl^- ion was necessary when a metal ion was bonded to the 2,4-dinitrobenzene substituted $\mathbf{L}_0$ in an exocyclic fashion. It is presumed, therefore, that attachment of electron withdrawing groups in $\mathbf{L}_1$–$\mathbf{L}_5$ imposes structural constraints and distorts the cryptand core for a favorable Cu(II) coordination, preferably from outside of the cavity, in presence of a coordinating solvent like MeCN when perchlorate salt is used or in a weakly or non-coordinating solvent to the system like THF when chloride salt is used (Scheme 2). This solvent assisted fluorescence recovery is rare in the literature.

Thus, occurrence of dual emissions in presence of Cu(II) in these ligands points to the fact that the metal ion engages the lone-pair on the N attached to the anthryl group and suppresses the operative PET resulting in fluorescence monomer enhancement while at the same time controlled movement of the side-arms attached to the cryptand core results in exciplex emission due to an intra-molecular π–π stacking interaction between the anthracene and electron-withdrawing groups.

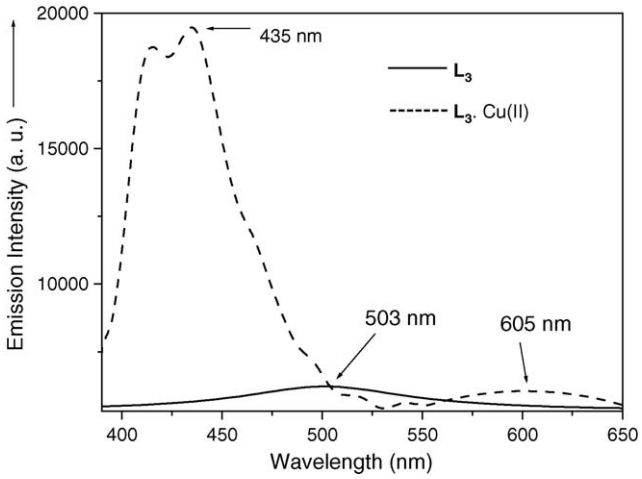

Fig. 8. Solid-state emission spectra of $\mathbf{L}_3$ and its Cu(II) complex.

Table 4
Solid-state emission (λ_{em}^{max}, nm) of the ligands $\mathbf{L}_1$–$\mathbf{L}_5$, their Cu(II) complexes as well as protonated species

Systems	Ligand λ_{em}^{max} (nm)	Cu(II) complexes		Protonated species	
		λ_{em}^{LE} (nm)	λ_{em}^{EX}(nm)	λ_{em}^{LE} (nm)	λ_{em}^{EX} (nm)
$\mathbf{L}_1$	538	558	664	544	665
$\mathbf{L}_2$	543	601	665	599	664
$\mathbf{L}_3$	503	435	605	457	624
$\mathbf{L}_4$	527	564	667	559	660
$\mathbf{L}_5$	517	538	649	533	646

3.7. Solid-state emission

The solid-state emission of Cu(II)/H^+ complexes of $\mathbf{L}_1$–$\mathbf{L}_5$ exhibit a prominent exciplex at 650–700 nm region in addition to the monomer emission at ~450–550 nm. The emission spectra of $\mathbf{L}_3$ and its Cu(II) complex exhibiting both monomer as well as exciplex emission is shown in Fig. 8. In the solid state, each ligand gives a low intensity emission in 500–550 nm region as well which may be due to ligand localized excimer or exciplex emission resulting from favorable non-bonded inter-molecular interactions in the packing of the molecules in the crystal lattice. The solid-state emission bands are collected in Table 4.

4. Conclusion

In conclusion, we show that structural modification to the cryptand receptor through attachment of electron-withdrawing 2,4-dinitrobenzene or 4-nitrobenzene results in fluorescence signaling systems that exhibit specificity towards Cu(II) with high fluorescence enhancement. It also results in the formation of an exciplex in a polar medium such as acetonitrile which is rare. The solvent assisted fluorescence recovery upon Cu(II) complexation suggests the participation of the acetonitrile molecules in Cu(II) binding from outside the cryptand cavity. The controlled movements of the attached side arms which accounts for the exciplex emission upon Cu(II) binding, may lead these supramolecular systems to act as a metal-ion driven

molecular machine operating with light input, if the movement can be operated in a reversible fashion. We are presently working along these lines.

Acknowledgement

Financial support for this work from the Department of Science and Technology, New Delhi is gratefully acknowledged.

Appendix A. Supplementary data

Supplementary data associated with this article can be found, in the online version, at 10.1016/j.jphotochem.2005.12.001.

References

[1] P. Ghosh, P.K. Bharadwaj, J. Roy, S. Ghosh, J. Am. Chem. Soc. 119 (1997) 11903.
[2] P.K. Bharadwaj, Prog. Inorg. Chem. 51 (2003) 251.
[3] G. Das, P.K. Bharadwaj, M.B. Roy, S. Ghosh, J. Photochem. Photobiol. A 135 (2000) 7.
[4] B. Bag, P.K. Bharadwaj, J. Lumin. 110 (2004) 85.
[5] R. Krämer, Angew. Chem. Int. Ed. 37 (1998) 772.
[6] K.A. Mitchell, R.G. Brown, D. Yuan, S.-C. Chang, R.E. Utecht, D.E. Lewis, J. Photochem. Photobiol. A 115 (1998) 157.
[7] V. Balzani, A. Credi, F.M. Raymo, J.F. Stoddart, Angew. Chem. Int. Ed. 39 (2000) 3348.
[8] For reviews, please see, Special issue on Molecular Machines, Acc. Chem. Res. 34 (2001) issue 6.
[9] B. Bag, P.K. Bharadwaj, Org. Lett. 7 (2005) 1573.
[10] J.B. Birks, Photophysics of Aromatic Molecules, Wiley-Interscience, New York, 1970.
[11] P. Ghosh, P.K. Bharadwaj, J. Chem. Soc.: Dalton Trans. (1997) 2673.
[12] P. Mukhopadhyay, P.K. Bharadwaj, A. Krishnan, P.K. Das, J. Mater. Chem. 12 (2002) 2786.
[13] M. Bullpit, W. Kitching, D. Doddrell, W. Adcock, J. Org. Chem. 41 (1976) 760.
[14] B. Bag, P.K. Bharadwaj, J. Chem. Sci. 117 (2005) 145.
[15] Crystal data for L_4: $C_{110}H_{112}N_{18}O_{22}Cl_{12}$; $M_w = 2463.58$; blocks; orange crystals, triclinic, space group P −1, $a = 10.725(5)$ Å, $b = 14.940(5)$ Å, $c = 18.779(5)$ Å, $\alpha = 79.606(5)^\circ$, $\beta = 82.045(5)^\circ$, $\gamma = 82.729(5)^\circ$, $U = 2915.2(8)$ Å^3, $T = 293$ K, $Z = 2$, μ(Mo Kα) = 0.362 mm^{-1}, $F(0\,0\,0) = 1278$, $\rho_{calc} = 1.403$ mg/m^3, 10135 reflection data with 757 parameters, 5863 [$I \geq 2\sigma(I)$] unique reflections were used in all calculations. The final R1 = 0.1040, WR2 = 0.3225, $S = 1.120$ (CCDC No. 282371). For crystal data of $\mathbf{L}_1$, $\mathbf{L}_2$, [$\mathbf{L}_1 \cdot \mathbf{H}^+$] and [$\mathbf{L}_2 \cdot \mathbf{2H}^+$], see Ref. [9]. The CCDC deposition numbers for crystal structures $\mathbf{L}_1$, $\mathbf{L}_2$, [$\mathbf{L}_1 \cdot \mathbf{H}^+$] and [$\mathbf{L}_2 \cdot \mathbf{2H}^+$] are CCDC 258795, 258796, 258797 and 258798, respectively.
[16] B. Ramachandram, A. Samanta, J. Phys. Chem. A 102 (1998) 10579.
[17] N.B. Sankaran, A. Das, A. Samanta, Chem. Phys. Lett. 351 (2002) 61.
[18] A. Horvath, K.L. Stevenson, Charge-Transfer Photochemistry of Coordination Compounds, VCH, Weinheim, Germany, 1993.
[19] M.B. Roy, S. Ghosh, P. Bandyopadhyay, P.K. Bharadwaj, J. Lumin. 92 (2001) 115.
[20] F. Fages, J.-P. Desvergne, H. Bouas-Laurent, P. Marsau, J.-M. Lehn, F. Kotzyba-Hibert, A.-M. Albrecht-Gary, M. Al-Joubbeh, J. Am. Chem. Soc. 111 (1989) 8672.
[21] H. Beens, A. Weller, Chem. Phys. Lett. 2 (1968) 140.
[22] A.P. de Silva, H.Q.N. Gunaratne, J. Habib-Jiwan, C.P. McCoy, T.E. Rice, J. Soumillion, Angew. Chem. Int. Ed. Engl. 34 (1995) 1728.
[23] H. Irving, R.J.P. Williams, J. Chem. Soc. (1953) 3192.
[24] M. Boiochhi, L. Fabbrizzi, M. Licchelli, D. Sachhi, M. Vázquez, C. Zampa, Chem. Commun. (2003) 1812.
[25] M.A. Bernardo, F. Pina, E. García-España, J. Latorre, S.V. Luis, J.M. Llinares, J.A. Ramírez, C. Soriano, Inorg. Chem. 37 (1998) 3935.
[26] M. Gordon, W.R. Ware (Eds.), The Exciplex, Academic Press Inc., New York, 1975.
[27] P. Mukhopadhyay, B. Sarkar, P.K. Bharadwaj, K. Nättinen, K. Rissanen, Inorg. Chem. 42 (2003) 4955.